Available online at www.sciencedirect.com
SCIENCE DIRECT
Biochemical and Biophysical Research Communications 345 (2006) 239–247
BBRC
www.elsevier.com/locate/ybbrc

The role of Paraxial Protocadherin in *Xenopus* otic placode development

Rui-Ying Hu, Peng Xu, Yue-Lei Chen, Xin Lou, Xiaoyan Ding *

Laboratory of Molecular Cell Biology, Institute of Biochemistry and Cell Biology, Shanghai Institutes for Biological Sciences, Chinese Academy of Sciences, Graduate School of the Chinese Academy of Sciences, 320 Yue Yang Road, Shanghai 200031, China

Received 14 April 2006
Available online 25 April 2006

Abstract

Vertebrate inner ear develops from its rudiment, otic placode, which later forms otic vesicle and gives rise to tissues comprising the entire inner ear. Although several signaling molecules have been identified as candidates responsible for inner ear specification and patterning, many details remain elusive. Here, we report that *Paraxial Protocadherin* (*PAPC*) is required for otic vesicle formation in *Xenopus* embryos. *PAPC* is expressed strictly in presumptive otic placode and later in otic vesicle during inner ear morphogenesis. Knockdown of *PAPC* by dominant-negative *PAPC* results in the failure of otic vesicle formation and the loss of early inner ear markers *Sox9* and *Tbx2*, suggesting the requirement of *PAPC* in the early stage of otic vesicle development. However, *PAPC* alone is not sufficient to induce otic placode formation.

Keywords: *PAPC*; Otic placode; Otic vesicle; Inner ear; *Sox9*; *Tbx2*; *Xenopus laevis*

In vertebrates, the first morphologically discernible structure during inner ear development is the otic placode, which arises from ectodermal thickenings at the border between the prospective hindbrain and the future epidermis [1,2]. The placode subsequently invaginates to form the otic cup and then the otic vesicle. Cells of otic vesicle undergo a distinct period of intense proliferation and complex morphogenetic movement prior to differentiation into specific cell types of the inner ear [1,3], including the mechanosensory hair cells that transmit balance and auditory information, supporting cells, and the biomineralized otoliths or otoconia that assist in perception [2]. Early inner ear morphogenesis accompanies otic placode specification and patterning.

Classical transplantation experiments have shown that inner ear formation is resulted from interactions between competent epidermal cells and adjacent tissues including the hindbrain and the paraxial mesoderm [1,2]. Studies in various species have implicated that signaling molecules of the FGF family [4–9], *Wnt8C* [9], retinoic acid [10,11], *Shh* [12–14] and the transcription factors like *Dlx* [4], *Pax2* [15], and *Sox9* [16] are involved in the specification and patterning of the inner ear in vertebrate embryos. In the mouse, mutations in some of these genes result in the loss of specific inner ear components, demonstrating the importance of these genes in this process [17].

Protocadherins constitute a large subgroup of the cadherin family, the calcium-dependent cell–cell adhesion molecules, which have functions in tissues of a wide variety of multicellular organisms [18,19]. Many of the protocadherins in mammals are strongly expressed in the central nervous system to modulate synaptic transmission and the generation of specific synaptic connections. Recently, their roles in tissue morphogenesis and formation of neuronal circuits during early vertebrate development have been inferred [18,19].

Xenopus Paraxial Protocadherin (*PAPC*), which was initially identified in a screen for genes present in the Spemann organizer of *Xenopus* embryos, is expressed during gastrulation and somitogenesis [20]. *PAPC* has homophilic adhesion properties and mediates selective cell–cell adhesion and cell sorting, ensuring cell movement during convergent extension (CE) in *Xenopus* and zebrafish [20,21].

* Corresponding author. Fax: +86 21 54921011.
E-mail address: xyding@sunm.shcnc.ac.cn (X. Ding).

0006-291X/$ - see front matter © 2006 Elsevier Inc. All rights reserved.
doi:10.1016/j.bbrc.2006.04.068

However, like other protocadherins, the cytoplasmic tail of *Xenopus PAPC* was largely different from the highly conserved cytoplasmic domain of the classical cadherins. It also has signaling functions besides adhesion properties. *Xenopus PAPC* acts through its cytoplasmic domain in cooperation with the Wnt/PCP pathway that modulates the activity of the small GTPases Rho A and Rac 1 and c-jun N-terminal kinase (JNK). This novel signaling function of *PAPC* is essential for the CE cell movements in *Xenopus* [22,23]. Moreover, the adhesion property becomes stronger when mutant form of *PAPC* lacking the cytoplasmic domains (*M-PAPC*) was tested, while similar deletions of the intracellular domain of classical cadherins cause loss of adhesion activity or even inhibition of cadherin adhesion [20]. These data strongly suggested a negative regulation of adhesion by the cytoplasmic domains of these protocadherins.

The distinctive feature of *PAPC* in both adhesiveness and signal transduction in gastrulation raises the question whether this also holds true in other developmental events. Here we report our observation of the dynamic *PAPC* expression during *Xenopus* inner ear development. We first show that *PAPC* is initiated in presumptive otic placode at the late neurula stage, prior to any morphological changes in the ectoderm, and later strictly expressed in otic placode throughout the otic vesicle formation. Results from loss-of-function experiments support the requirement of *PAPC* for otic placode specification in *Xenopus*. However, *PAPC* alone is not sufficient to induce otic placode formation.

Materials and methods

Embryo manipulation and microinjection. Xenopus laevis fertilized eggs were obtained, dejellied and cultured as previously described [24], and staged according to Nieuwkoop and Faber [25]. Synthetic RNA mixed with β-galactosidase mRNA was injected into one of the two animal ventral cells to target the otic placode territory at the eight-cell stage [16] or one of the two blastomeres at the two-cell stage [12]. Embryos were collected at stage 32 (tailbud stage) and fixed in MEMFA. After X-gal staining for β-galactosidase acitivity as previously described [26], embryos were transferred to methanol and prepared for in situ hybridization.

In vitro transcription of capped mRNAs and in situ hybridization probes. mRNA for microinjection and probes for in situ hybridization were prepared as previously described [24]. To obtain sense mRNA, *FL-PAPC* (a kind gift of Dr. Eddy M. De Robertis) [20], *M-PAPC* (a kind gift of Dr. Herbert Steinbeisser) [20], *DN-PAPC* (a kind gift of Dr. Herbert Steinbeisser) [20], and β-galactosidase were digested with *Not*I and transcribed with SP6 RNA polymerase. Antisense digoxigenin-labeled probes were synthesized using linearized template encoding *PAPC*[20], *Sox9*[16], and *Tbx2*[27].

RT-PCR. RNA isolation and reverse transcription were performed as described [24]. For each experiment, the quantity of input cDNA was determined by normalization of the *ODC* signal. The primers used for *ODC* were: forward, 5′ GATCATGCACATGTCAAGCC 3′ and reverse, 5′ CAGGGAGAATGCCATGTTCT 3′ (58 °C, 25 cycles) [28]. The primers used for *PAPC* were: forward, 5′ CGTCTAGCAGATACCA AGAATTC 3′ and reverse, 5′ GCTAGTTAGGTGACAGGACAATG 3′ (58 °C, 30 cycles).

Whole-mount in situ hybridization and bleaching. Whole-mount in situ hybridization was carried out with antisense digoxigenin-labeled probes, using a modification of the protocol described by Dietrich et al. [29]. After in situ staining, the embryos were dehydrated in methanol, bleached in methanol/37% H_2O_2 (2:1, V/V) in daylight or under UV irradiation. Samples were then hydrated in 1× PBS and photographed under Leica MZFL-III microscope. For sectioning, samples were overstained by in situ hybridizations and embedded in paraffin, sectioned at 10 μm thickness.

Results

PAPC is expressed in the developing otic placode

In an investigation of *PAPC* function during somitogenesis, we noticed a phenomenon that *PAPC* also had strong expression in otic placode. As the first step toward understanding the role of *Xenopus PAPC* during inner ear development, we used RT-PCR to define its temporal expression in *Xenopus* embryos. In *Xenopus*, the inner ear begins as an otic placode in the stage 23 embryos. This placode invaginates and forms a closed vesicle that is completely separated from the overlying epidermis at stage 28 [30]. Since *PAPC* was also expressed at the paraxial mesoderm in the same stage of otic placode formation, RT-PCR with cDNA derived from head of various stages embryos was performed (Fig. 1B). The *PAPC* transcription level was high from stage 21, before the otic placode is visible, to stage 33, when the otic vesicle formed, while it slightly decreased from stage 37 and still expressed at stage 45 (Fig. 1A).

In *Xenopus* embryos, presumptive otic placode ectoderm is specified to form otic placode by the neurula stage [31]. To visualize the spatial expression patterns of *Xenopus PAPC* in the otic placode and vesicle, we then performed whole-mount in situ hybridization with a digoxigenin-labeled RNA probe for *PAPC*. At stage 17 (late neurula stage), *PAPC* was detected in bilateral patches of cells (red arrow, Fig. 2A) immediately adjacent to the lateral neural crest and corresponding to the prospective otic

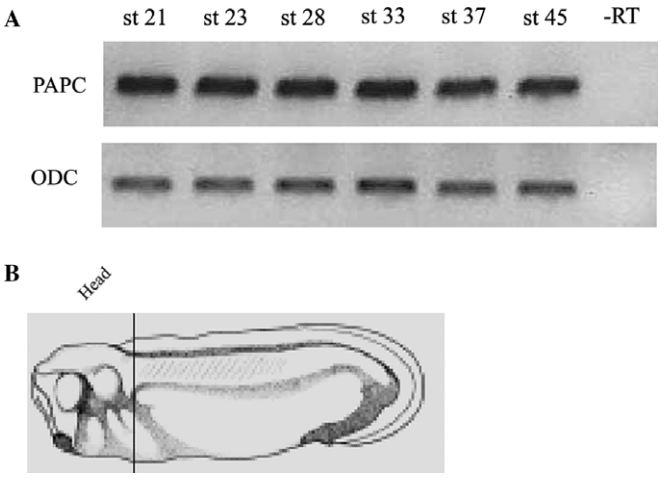

Fig. 1. Expression profile of *PAPC* in *Xenopus* head analyzed by RT-PCR. (A) Total RNA extracted from dissected head of stage 21–45 embryos was reverse transcribed and PCR amplified using *PAPC*-specific primers. *PAPC* transcripts were present at each stage of otic placode development. (B) Vertical line indicates the position to dissect heads of stage 21–45 embryos.

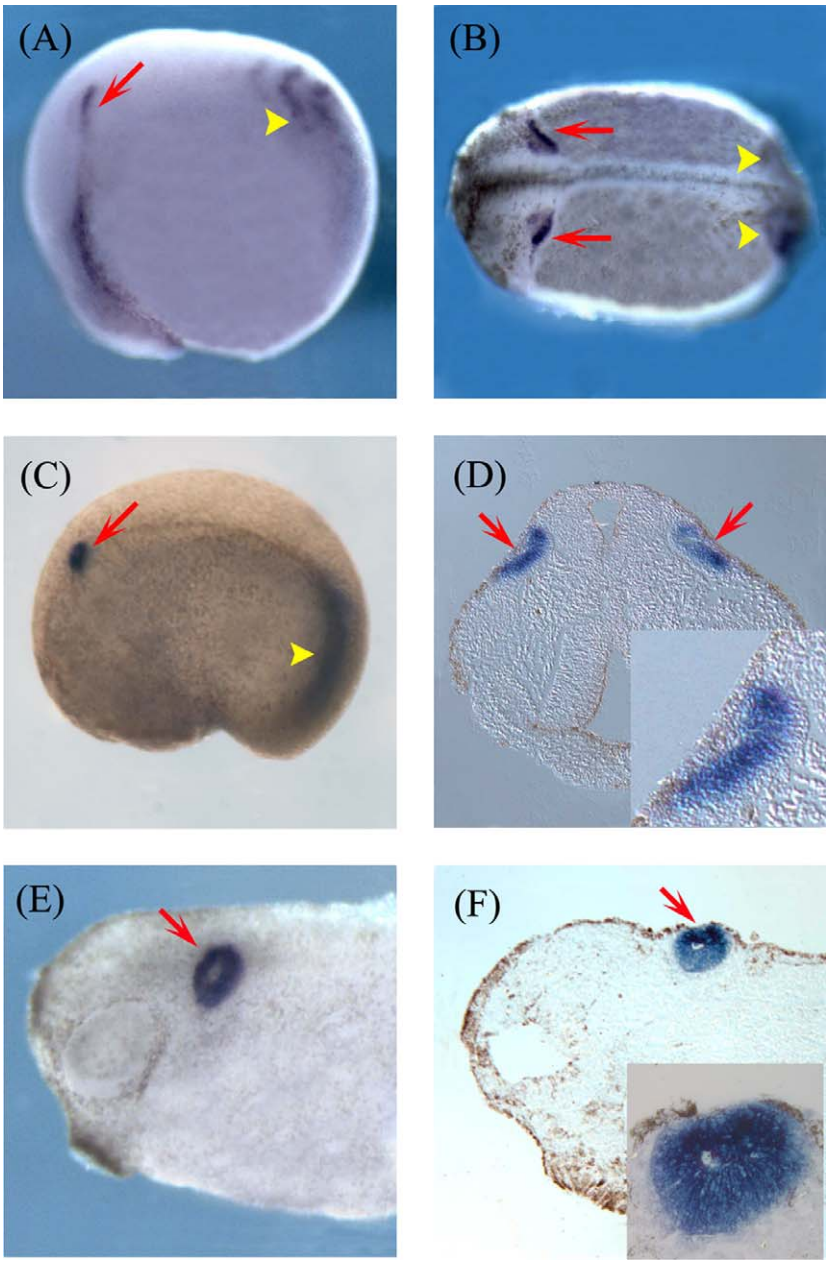

Fig. 2. Spatial localization of *Xenopus PAPC* transcripts during inner ear development visualized by whole-mount in situ hybridization analysis. Transcripts for *PAPC* were detected by whole-mount in situ hybridization. (A,C,D) Lateral views are shown with anterior to the left. (B) Dorsal view with anterior to the left. (A) In late neurula (stage 17), bilateral stripes of *PAPC* expression prefigured the prospective otic placode. *PAPC* expression was also found in the forming somite. (B) At stage 20, *PAPC* was expressed in the prospective otic placode. (C) At stage 23, the expression of *PAPC* was in the otic cup. (D) A transverse section of a stage 23 embryo revealed *PAPC* transcripts were present in the otic cup. Insertion is the enlargement of (D). (E) At the hatching stage (stage 32), *PAPC* was clearly expressed in the otic vesicles. (F) A transverse section through the hindbrain region of a stage 32 embryo. *PAPC* transcripts were detected in the entire otic vesicle. Insertion is the enlargement of (F). Red arrows indicate the otic signal; yellow arrowheads indicate the signals in the posterior region.

placode. As development proceeds, *PAPC* transcripts were restrictively localized in the developing otic placode cells throughout the invagination phase (Fig. 2B and C). At stage 20, *PAPC* expression in prospective otic placode was even stronger than those in the posterior region (paraxial mesoderm, Fig. 2B), consistent with our RT-PCR results (data not shown). After the shaping of otic placode in the stage 23, *PAPC* expressions became more coherent and restricted to the otic cup, as illustrated by transverse section of a stage 23 embryo (Fig. 2D). This inner ear specific expression pattern was continued in advanced stages (Fig. 2E). Section through the hindbrain region of a stage 32 embryo showed strong signals (Fig. 2F, red arrow) in otic vesicle. Taken together, we conclude that *PAPC* is dynamically expressed in inner ear cells undergoing morphogenesis during otic placode development. The tight

coupling of *PAPC* expression and otic vesicle formation indicate that *PAPC* may play a central role in auditory system development, by means of cell sorting and cell fate decision.

PAPC depletion disrupts otic vesicle formation

In order to address the potential function of *PAPC* during otic cell fate decision and morphogenesis, we performed loss-of-function studies using dominant-negative *PAPC* (*DN-PAPC*) or membrane-tethered forms of *PAPC* (*M-PAPC*) to interfere with *PAPC* function. *DN-PAPC* plasmid encodes a secreted extracellular domain of *PAPC* which lacks both the transmembrane domain and the intracellular C-terminus. *M-PAPC* lacks most of the intracellular C-terminus but still possesses the transmembrane domain [20]. The validity of these constructs was pre-tested by the in vivo cell adhesion assay as described by Kim et al. [20] (data not shown). Capped *DN-PAPC* mRNA or *M-PAPC* mRNA together with a lineage tracer β-galactosidase was microinjected into the right side animal ventral blastomere of the eight-cell stage embryos which is destined to the otic placode territory [16]. As the *PAPC*-depleted embryos reached the hatching stage (stage 32), they displayed severe otic vesicle defects in the injected side ($n = 40$, 85% for *DN-PAPC* injection and $n = 28$, 86% for *M-PAPC* injection, respectively) (Fig. 3B and D), while the control side remained normal ($n = 68$, 100%) (Fig. 3A and C). In contrast, embryos injected with β-galactosidase only did not display any defects (data not shown). Furthermore, we observed some pigmented cells aggregated in the injected side (Fig. 3B and D, red arrowhead). This defect was more severe in *DN-PAPC* injected embryos than that in *M-PAPC* injected ones. It seemed that these cells did not migrate to the proper position of the destined otic placode.

PAPC depletion prevents the expression of otic vesicle markers

To further elucidate whether loss-of-*PAPC*-function has any effect on otic cell fate decision, we analyzed the expression pattern of two otic marker genes *Sox9* and *Tbx2* in the manipulated embryos. *Sox9* seems to be the earliest specific marker for the otic placode in *Xenopus*, whose expression could be first detected in prospective otic placode ectoderm at late gastrula stage (stage 12.5). As the otic cup invaginates to form a vesicle, *Sox9* is expressed throughout the otic vesicle at

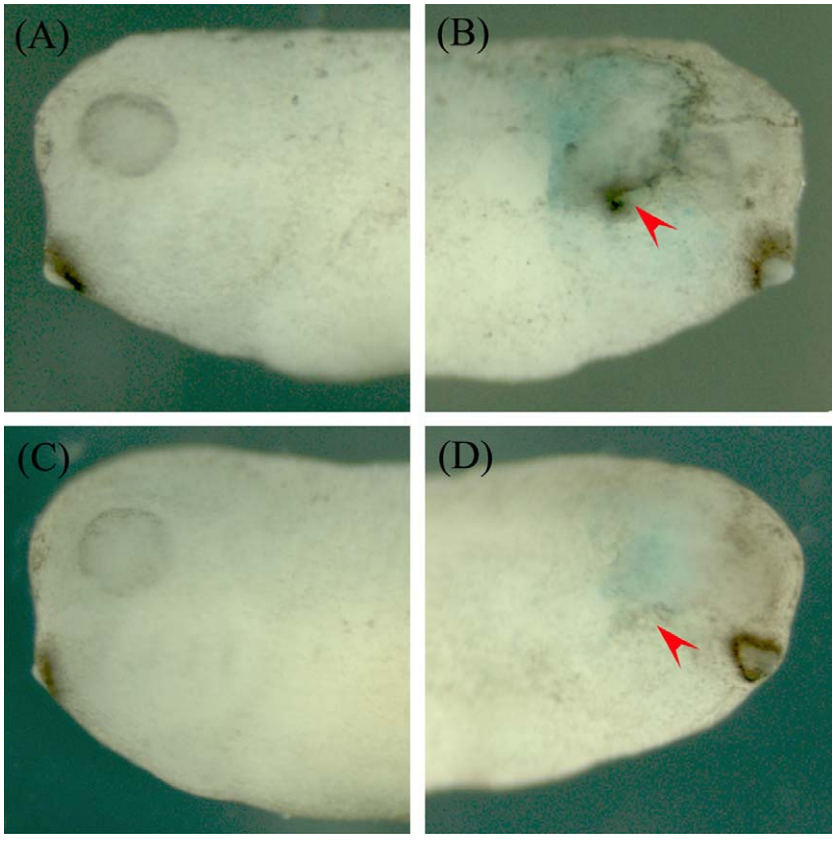

Fig. 3. Reduction of *PAPC* disrupts the otic vesicle structure. (A,B) Otic vesicle was lost in the embryos when 1.5 ng *DN-PAPC* and 200 pg β-galactosidase were injected in the right side animal ventral blastomere at the eight-cell stage ($n = 40$, 85%). (C,D) Otic vesicle was lost in the embryos injected with 400 pg *M-PAPC* and 200 pg β-galactosidase in the right side animal ventral blastomere at the eight-cell stage ($n = 28$, 86%). (A,C) Control side. (B,D) Injected side. (B) Pigmented cells aggregated in the injected side (red arrowhead). (D) A few pigmented cells aggregated in the injected area (red arrowhead). Blue color domain is LacZ staining.

tailbud stage [16]. *Tbx2* is another otic marker, expressed throughout the entire otic vesicle in swimming larvae [27]. *Sox9* and *Tbx2* expression was lost when either *DN-PAPC* (Fig. 4B and E) or *M-PAPC* (Fig. 4H and K) was injected into the right side animal ventral blastomere of eight-cell stage embryos. By contrasts, the expression of both genes was unperturbed in uninjected control sides (Fig. 4A, D, G, and J).

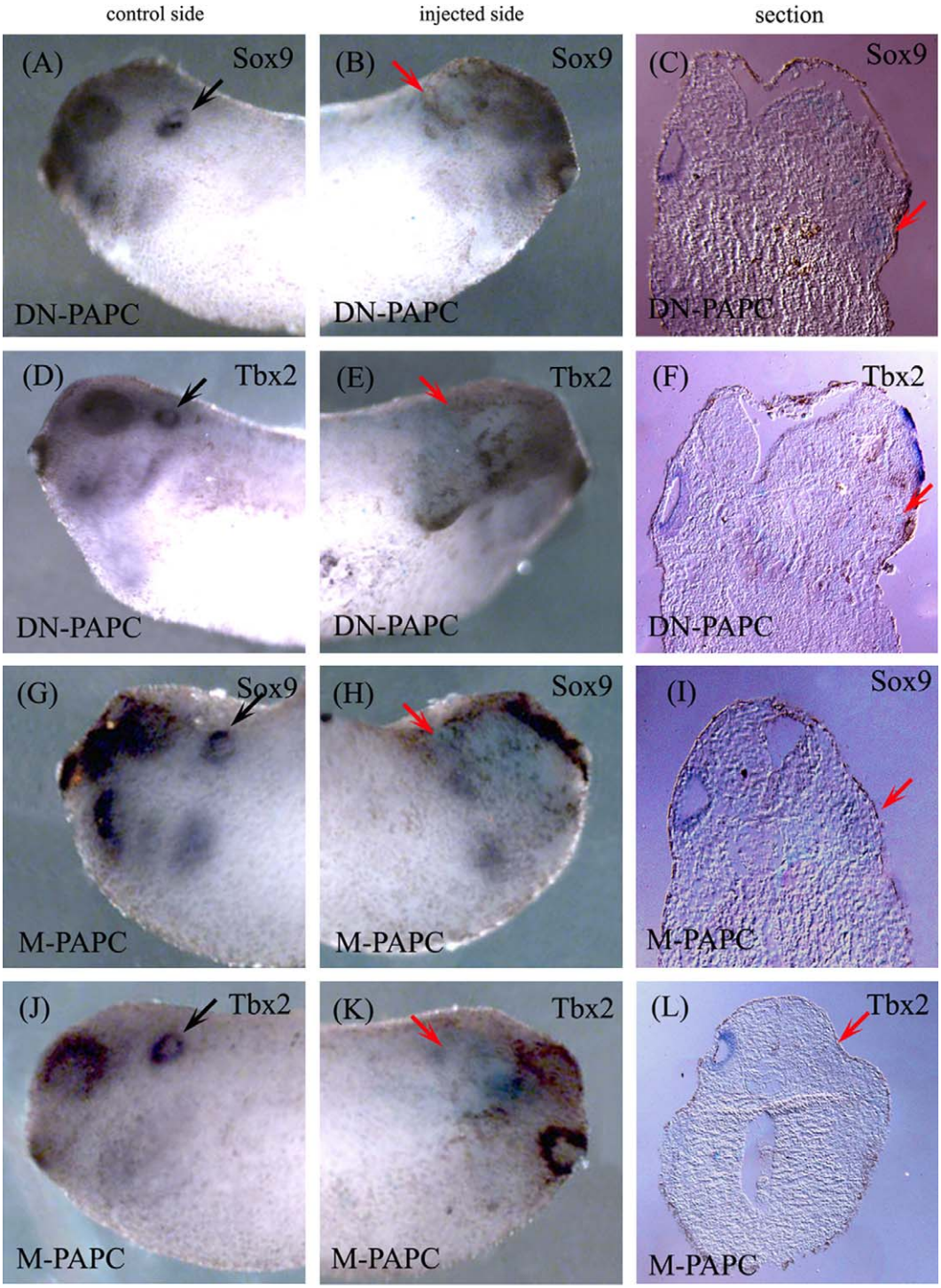

Fig. 4. *PAPC* is required to specify the otic placode. Expression of *Sox9* and *Tbx2* in *DN-PAPC* or *M-PAPC* injected embryos in stage 32, detected by whole-mount in situ hybridization. (A–F) *Sox9* and *Tbx2* expression was both lost in embryos injected with 1.5 ng *DN-PAPC* in the right side animal ventral blastomere at the eight-cell stage. (A,B,C) *Sox9* expression ($n = 22$, 86%). (D,E,F) *Tbx2* expression ($n = 18$, 83%). (G–L) *Sox9* and *Tbx2* expression was both lost in embryos injected with 400 pg *M-PAPC* in the right side animal ventral blastomere at the eight-cell stage. (G,H,I) *Sox9* expression ($n = 15$, 86%). (J,K,L) *Tbx2* expression ($n = 13$, 85%). (A,D,G,J) Control side. (B,E,H,K) Injected side. (C,F,I,L) Transverse section through the embryo injected with either 1.5 ng *DN-PAPC* or 400 pg *M-PAPC*. Black arrows indicate the positive signal; red arrows indicate the absence of the signal in the injected side.

Moreover, sagittal section through *DN-PAPC*-injected embryos revealed that most of these embryos lacked a recognizable otic vesicle on the injected side, while the overall morphology of these embryos was otherwise unperturbed (Fig. 4C and F). Similar results were obtained with *M-PAPC* (Fig. 4I and L).

In order to investigate whether the phenotypes of *DN-PAPC* or *M-PAPC* injection were indeed caused by the inhibition of *PAPC* function, in vivo rescue experiments were performed by co-injection with *FL-PAPC*. Capped *FL-PAPC* mRNA capable of forming functional protein in *Xenopus* embryos (data not shown) was co-injected with either *DN-PAPC* mRNA or *M-PAPC* mRNA into the right side animal ventral blastomere of the eight-cell stage embryos. Indeed, the defects of otic vesicle structure and otic marker gene *Tbx2* expression caused by *DN-PAPC* or *M-PAPC* injection can be rescued by co-injection of *FL-PAPC* (Fig. 5B and D). Co-injecting

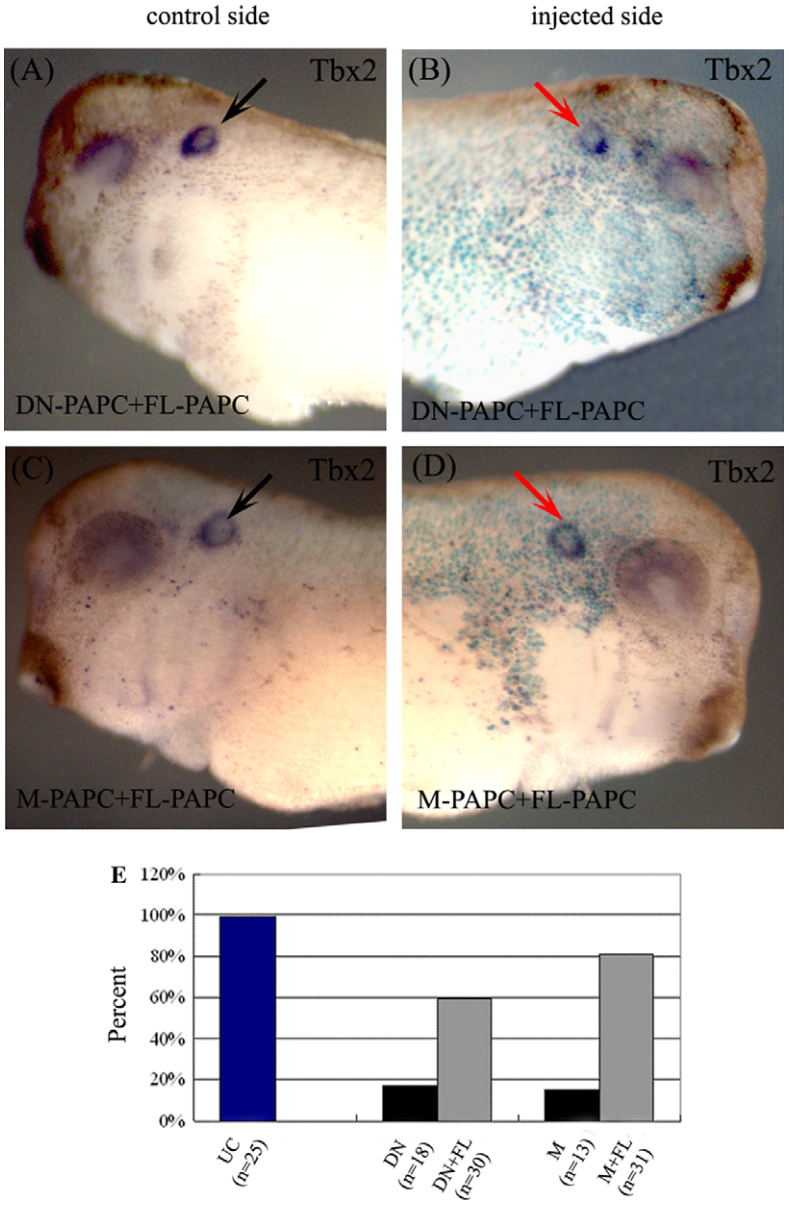

Fig. 5. Co-injection of *FL-PAPC* rescues the otic vesicle defects. Defects of otic vesicle formation and *Tbx2* expression are rescued by *FL-PAPC* co-injected with either *DN-PAPC* or *M-PAPC*, detected by whole-mount in situ hybridization in stage 32 embryos. (A,B) Otic vesicle and *Tbx2* expression was rescued in embryos co-injected with 1 ng *FL-PAPC* and 1.5 ng *DN-PAPC* in the right side animal ventral blastomere at the eight-cell stage ($n = 30$, 60%). (C,D) Otic vesicle and *Tbx2* expression was rescued in embryos co-injected with 1 ng *FL-PAPC* and 400 pg *M-PAPC* in the right side animal ventral blastomere at the eight-cell stage ($n = 31$, 81%). (A,C) Control side. (B,D) Injected side. Black arrows indicate the endogenous positive signal; red arrows indicate the rescued signal in the injected side. (E) *Tbx2* expression rescued by co-injection with *FL-PAPC*. The blue bar depicts the percentage of uninjected sibling embryos; the black bar depicts the percentage of embryos injected with either *DN-PAPC* or *M-PAPC*; the dark gray bar depicts the percentage of embryos co-injected of *FL-PAPC* with either *DN-PAPC* or *M-PAPC*. UC, uninjected sibling control embryos; DN, *DN-PAPC*; M, *M-PAPC*; FL, *FL-PAPC*.

FL-PAPC with either *DN-PAPC* or *M-PAPC* decreased the number of embryos with reduced *Tbx2* expression from 83% to 40% (*DN-PAPC*) and from 85% to 19% (*M-PAPC*), respectively (Fig. 5E).

The morphological abnormality and absence of expression of two otic marker genes in *PAPC* depleted embryos suggest that not only inner ear morphogenesis but also otic cell fate decision requires *PAPC* function.

PAPC is not sufficient to induce otic placode formation

As the loss-of-function studies indicate that *PAPC* was required for otic vesicle formation, and the rescue experiments indicated the *FL-PAPC* could exert its function in vivo, we then sought to investigate whether *PAPC* alone could initiate an otic placode in a gain-of-function situation. To misexpress *PAPC*, capped *FL-PAPC* mRNA together with β-galactosidase were microinjected into one of two blastomeres at two-cell stage embryos, a circumstance sufficient for induction of ectopic inner ears [12]. In all of the injected embryos at tailbud stage ($n = 26$, 100%), we did not observe the formation of morphologically distinct circular shaped inner ear structures. To examine the effects of ectopic expressed *PAPC*, we then analyzed two otic markers *Sox9* and *Tbx2* in *FL-PAPC* injected embryos by whole-mount in situ hybridization. As shown in Fig. 6, ectopic expression of *FL-PAPC* mRNA did not induce ectopic *Sox9* ($n = 14$, 100%) (Fig. 6A) or *Tbx2* ($n = 12$, 100%) expression (Fig. 6B).

These results give strong suggestion that *PAPC* alone cannot directly induce otic placode formation.

Discussion

The important roles of *PAPC* in CE movements during gastrulation [20,21] and segmental boundaries formation during somitogenesis [32–34] were demonstrated by loss-of-function experiment in *Xenopus*. It was also mentioned that *PAPC* could be detected in the forming otic vesicle but no temporal-spatial expression pattern has been shown [20]. In this study, by careful analysis of the dynamic expression and loss- or gain-of-function of *PAPC* experiments, we present evidences that the adhesion molecule *PAPC* is required for the otic placode development in *Xenopus* embryos. This is supported by two observations: (1) *PAPC* is expressed in the presumptive otic placode before it becomes morphologically distinct and along with otic placode development; (2) depletion of *PAPC* by *DN-PAPC* or *M-PAPC* results in a loss of expression of two otic markers and a failure to form a recognizable otic vesicle.

Interestingly, we observed that otic-specific expression of *PAPC* occurs very early in embryogenesis, well before these otic structures become morphologically discernible. This observation strongly implies that *PAPC* is involved in otic cell fate decision. The distinctive otic-specific *PAPC* expression in advanced stages further supports this consideration. However, according to the misexpression experiments it seems that *PAPC* is not sufficient to induce otic placode formation. The translation of functional *PAPC* protein in our system was pre-tested (data not shown). So that we deduce that additional inductive signals synergize *PAPC* to induce the otic placodes.

The cytoplasmic tails of protocadherins were largely different from each other and from the highly conserved cytoplasmic domain of the classical cadherins. It has been demonstrated that the C-termini of various protocadherins can interact with components of signaling pathways such as Fyn tyrosine kinase [35], protein phosphatase 1 (PP1) [36], and the adapter molecule disabled-1 [37]. *PAPC* can also modulate the activity of the Rho GTPase and JNK, two regulators of the cytoskeletal architecture and effectors of the planar cell polarity pathway via its C-terminal [22,23]. The loss-of-function data of both *DN-PAPC* and *M-PAPC* presented in this current report suggested that *PAPC* might also function via its cytoplasmic tails as a signal factor for inner ear development in *Xenopus*.

The requirement of *PAPC* for otic vesicle development in *Xenopus* raises the possibility that other protocadherin

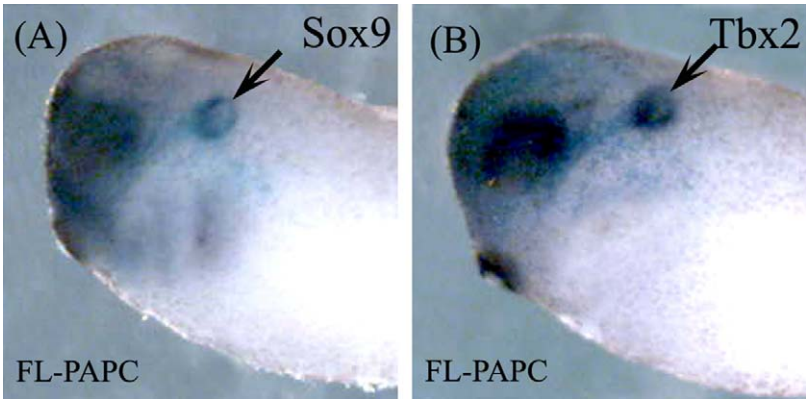

Fig. 6. *PAPC* is not sufficient to initiate formation of the otic placode. Embryos injected with *FL-PAPC* (800 pg) and β-galactosidase (200 pg) mRNA into one of two blastomeres at two-cell stage, fixed, and stained for expression of *Sox9* (A) and *Tbx2* (B) at stage 32. (A) Microinjection of *FL-PAPC* did not induce ectopic *Sox9* expression ($n = 14$, 100%). (B) Microinjection of *FL-PAPC* did not induce ectopic *Tbx2* expression ($n = 12$, 100%). Black arrows indicate the endogenous positive signal.

family members might be involved in the differentiation and the patterning of the otic vesicle. *Protocadherin 15 (PCDH15)* null mutant cause 'Ames waltzer' (av) mice, with deafness as a main phenotype, probably resulting from degeneration of the inner ear neuroepithelium and vestibular dysfunction [38]. *PCDH15* is the human homolog and was proposed as a candidate for Usher syndrome 1F (USH1F). Three different mutant alleles of *PCDH15* from four families segregating USH1F [39] were recently reported. Further investigation is required to interpret how these protocadherins interplay in otic development.

We also observed eye defects in some cases of *PAPC* depleted embryos. Although *DN-PAPC* or *M-PAPC* mRNA injection was performed according to the accurate fate map, it would also affect cells of the other cranial placodes including lens placode. In order to exclude this influence, we are going to use inducible inhibitory mutant *PAPC* construct to determine the time window during which *PAPC* is required for otic placode development.

Acknowledgments

We thank Dr. Eddy M. De Robertis for kindly providing us *FL-PAPC* and Dr. Herbert Steinbeisser for *DN-PAPC* and *M-PAPC* constructs. We thank Dr. Jean-Pierre Saint-Jeannet for the in situ hybridization probes (respectively, *Sox9* and *Tbx2*). We thank Dr. Shuang-Wei Li for critical reading of the manuscript. This work was supported by National Natural Science Foundation of China (30500276) to R.-Y.H., National Natural Science Foundation of China (90408005, 30270650) and the National Key Project for Basic Science Research of China (2001CB509901) to X.D.

References

[1] M. Torres, F. Giraldez, The development of the vertebrate inner ear, Mech. Dev. 71 (1998) 5–21.
[2] C.V. Baker, M. Bronner-Fraser, Vertebrate cranial placodes I. Embryonic induction, Dev. Biol. 232 (2001) 1–61.
[3] D.M. Fekete, Cell fate specification in the inner ear, Curr. Opin. Neurobiol. 6 (1996) 533–541.
[4] K.S. Solomon, S.J. Kwak, A. Fritz, Genetic interactions underlying otic placode induction and formation, Dev. Dyn. 230 (2004) 419–433.
[5] U. Pirvola, X. Zhang, J. Mantela, D.M. Ornitz, J. Ylikoski, Fgf9 signaling regulates inner ear morphogenesis through epithelial-mesenchymal interactions, Dev. Biol. 273 (2004) 350–360.
[6] D. Liu, H. Chu, L. Maves, Y.L. Yan, P.A. Morcos, J.H. Postlethwait, M. Westerfield, Fgf3 and Fgf8 dependent and independent transcription factors are required for otic placode specification, Development 130 (2003) 2213–2224.
[7] Y. Alvarez, M.T. Alonso, V. Vendrell, L.C. Zelarayan, P. Chamero, T. Theil, M.R. Bosl, S. Kato, M. Maconochie, D. Riethmacher, T. Schimmang, Requirements for FGF3 and FGF10 during inner ear formation, Development 130 (2003) 6329–6338.
[8] M. Adamska, H. Herbrand, M. Adamski, M. Kruger, T. Braun, E. Bober, FGFs control the patterning of the inner ear but are not able to induce the full ear program, Mech. Dev. 109 (2001) 303–313.
[9] R.K. Ladher, K.U. Anakwe, A.L. Gurney, G.C. Schoenwolf, P.H. Francis-West, Identification of synergistic signals initiating inner ear development, Science 290 (2000) 1965–1967.
[10] M. Pasqualetti, R. Neun, M. Davenne, F.M. Rijli, Retinoic acid rescues inner ear defects in Hoxa1 deficient mice, Nat. Genet. 29 (2001) 34–39.
[11] V. Dupe, N.B. Ghyselinck, O. Wendling, P. Chambon, M. Mark, Key roles of retinoic acid receptors alpha and beta in the patterning of the caudal hindbrain, pharyngeal arches and otocyst in the mouse, Development 126 (1999) 5051–5059.
[12] K. Koebernick, T. Hollemann, T. Pieler, A restrictive role for Hedgehog signalling during otic specification in *Xenopus*, Dev. Biol. 260 (2003) 325–338.
[13] M.M. Riccomagno, L. Martinu, M. Mulheisen, D.K. Wu, D.J. Epstein, Specification of the mammalian cochlea is dependent on sonic hedgehog, Genes Dev. 16 (2002) 2365–2378.
[14] W. Liu, G. Li, J.S. Chien, S. Raft, H. Zhang, C. Chiang, D.A. Frenz, Sonic hedgehog regulates otic capsule chondrogenesis and inner ear development in the mouse embryo, Dev. Biol. 248 (2002) 240–250.
[15] M. Torres, E. Gomez-Pardo, P. Gruss, Pax2 contributes to inner ear patterning and optic nerve trajectory, Development 122 (1996) 3381–3391.
[16] N. Saint-Germain, Y.H. Lee, Y. Zhang, T.D. Sargent, J.P. Saint-Jeannet, Specification of the otic placode depends on Sox9 function in *Xenopus*, Development 131 (2004) 1755–1763.
[17] D.M. Fekete, Development of the vertebrate ear: insights from knockouts and mutants, Trends Neurosci. 22 (1999) 263–269.
[18] S.T. Suzuki, Recent progress in protocadherin research, Exp. Cell Res. 261 (2000) 13–18.
[19] M. Frank, R. Kemler, Protocadherins, Curr. Opin. Cell Biol. 14 (2002) 557–562.
[20] S.H. Kim, A. Yamamoto, T. Bouwmeester, E. Agius, E.M. Robertis, The role of paraxial protocadherin in selective adhesion and cell movements of the mesoderm during *Xenopus* gastrulation, Development 125 (1998) 4681–4690.
[21] A. Yamamoto, S.L. Amacher, S.H. Kim, D. Geissert, C.B. Kimmel, E.M. De Robertis, Zebrafish paraxial protocadherin is a downstream target of spadetail involved in morphogenesis of gastrula mesoderm, Development 125 (1998) 3389–3397.
[22] A. Medina, R.K. Swain, K.M. Kuerner, H. Steinbeisser, *Xenopus* paraxial protocadherin has signaling functions and is involved in tissue separation, EMBO J. 23 (2004) 3249–3258.
[23] F. Unterseher, J.A. Hefele, K. Giehl, E.M. De Robertis, D. Wedlich, A. Schambony, Paraxial protocadherin coordinates cell polarity during convergent extension via Rho A and JNK, EMBO J. 23 (2004) 3259–3269.
[24] P.F. Fang, R.Y. Hu, X.Y. He, X.Y. Ding, Multiple signaling pathways control Tbx6 expression during *Xenopus* myogenesis, Acta Biochim. Biophys. Sin. (Shanghai) 36 (2004) 390–396.
[25] P.D. Niewkoop, J. Faber, Normal Table of *Xenopus laevis* (Daudin), Garland publishing Inc., New York, NY, 1994.
[26] H.L. Sive, R.M. Grainger, R.M. Harland, Early Development of *Xenopus laevis*: A Laboratory Manual, Cold Spring Harbor Laboratory Press, New York, 2000.
[27] Y. Takabatake, T. Takabatake, K. Takeshima, Conserved and divergent expression of T-box genes Tbx2-Tbx5 in *Xenopus*, Mech. Dev. 91 (2000) 433–437.
[28] T. Bassez, J. Paris, F. Omilli, C. Dorel, H.B. Osborne, Post-transcriptional regulation of ornithine decarboxylase in *Xenopus laevis* oocytes, Development 110 (1990) 955–962.
[29] S. Dietrich, F.R. Schubert, A. Lumsden, Control of dorsoventral pattern in the chick paraxial mesoderm, Development 124 (1997) 3895–3908.
[30] M.M. Bever, Y.Y. Jean, D.M. Fekete, Three-dimensional morphology of inner ear development in *Xenopus laevis*, Dev. Dyn. 227 (2003) 422–430.
[31] B.C. Gallagher, J.J. Henry, R.M. Grainger, Inductive processes leading to inner ear formation during *Xenopus* development, Dev. Biol. 175 (1996) 95–107.
[32] S.H. Kim, W.C. Jen, E.M. De Robertis, C. Kintner, The protocadherin PAPC establishes segmental boundaries during somitogenesis in *Xenopus* embryos, Curr. Biol. 10 (2000) 821–830.

[33] A. Yamamoto, C. Kemp, D. Bachiller, D. Geissert, E.M. De Robertis, Mouse paraxial protocadherin is expressed in trunk mesoderm and is not essential for mouse development, Genesis 27 (2000) 49–57.
[34] J. Rhee, Y. Takahashi, Y. Saga, J. Wilson-Rawls, A. Rawls, The protocadherin papc is involved in the organization of the epithelium along the segmental border during mouse somitogenesis, Dev. Biol. 254 (2003) 248–261.
[35] N. Kohmura, K. Senzaki, S. Hamada, N. Kai, R. Yasuda, M. Watanabe, H. Ishii, M. Yasuda, M. Mishina, T. Yagi, Diversity revealed by a novel family of cadherins expressed in neurons at a synaptic complex, Neuron 20 (1998) 1137–1151.
[36] K. Yoshida, M. Watanabe, H. Kato, A. Dutta, S. Sugano, BH-protocadherin-c, a member of the cadherin superfamily, interacts with protein phosphatase 1 alpha through its intracellular domain, FEBS Lett. 460 (1999) 93–98.
[37] R. Homayouni, D.S. Rice, T. Curran, Disabled-1 interacts with a novel developmentally regulated protocadherin, Biochem. Biophys. Res. Commun. 289 (2001) 539–547.
[38] K.N. Alagramam, C.L. Murcia, H.Y. Kwon, K.S. Pawlowski, C.G. Wright, R.P. Woychik, The mouse Ames waltzer hearing-loss mutant is caused by mutation of Pcdh15, a novel protocadherin gene, Nat. Genet. 27 (2001) 99–102.
[39] Z.M. Ahmed, S. Riazuddin, S.L. Bernstein, Z. Ahmed, S. Khan, A.J. Griffith, R.J. Morell, T.B. Friedman, S. Riazuddin, E.R. Wilcox, Mutations of the protocadherin gene PCDH15 cause Usher syndrome type 1F, Am. J. Hum. Genet. 69 (2001) 25–34.